Supporting information

Precisely Controlled Low-Valent Nickel Sites in Planar Polyphthalocyanine for Enhanced Urea Oxidation

Lu Zhao[1, *], Hui Tu[1], Liping Lin[1], Kai Chen[2], Bin Wu[1], Bing Sun[3], Weiyi Ge[1], Chaoqun Chang[1], Linbo Huang[1, *], Qi An[1]

1 Engineering Research Center of Ministry of Education for Geological Carbon Storage and Low Carbon Utilization of Resources, Beijing Key Laboratory of Materials Utilization of Nonmetallic Minerals and Solid Wastes, National Laboratory of Mineral Materials, Hebei Key Laboratory of Resource Low-carbon Utilization and New Materials, School of Materials Science and Technology, China University of Geosciences (Beijing), 100083, China

2 National Synchrotron Radiation Laboratory and School of Nuclear Science and Technology, University of Science and Technology of China, Hefei, 230026, China

3 School of Science, China University of Geosciences (Beijing), Beijing 100083, China

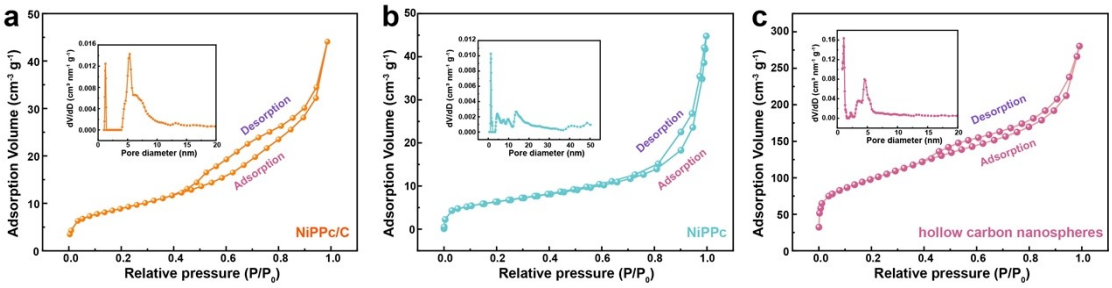

Figure S1. N_2 desorption/adsorption isotherms and pore size distribution curves calculated by the DFT model of (a) NiPPc/C, (b) NiPPc, and hollow carbon nanospheres.

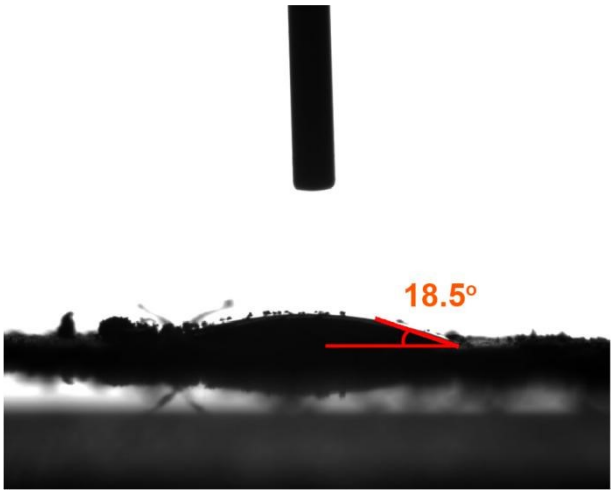

Figure S2. Contact angle tests of NiPPc/C.

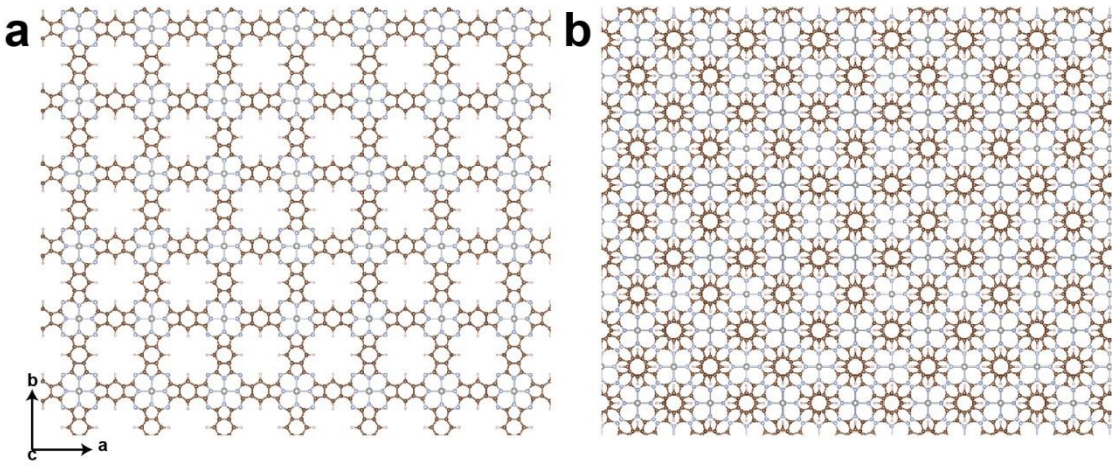

Figure S3. The calculated crystal structure of (a) AA-stacking NiPPc with a P4/MMM space group (a = b = 10.57880 Å, c = 3.0440 Å, α = β = γ = 90°.) and (b) AB-stacking NiPPc with an I4/MMM space group (a = b = 10.97987 Å, c = 5.189102 Å, α = β = γ = 90°).

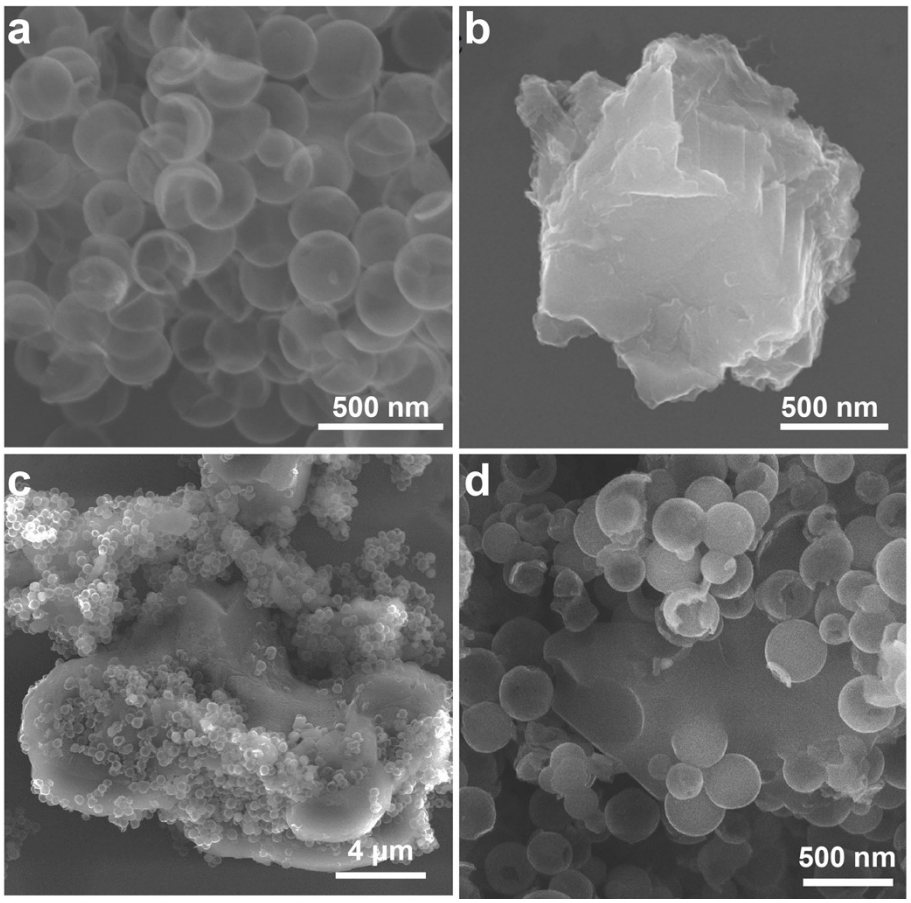

Figure S4. SEM images of (a) hollow carbon nanospheres, (b) NiPPc, (c) NiPPc/$C_{0.6}$ and (d) NiPPc/C.

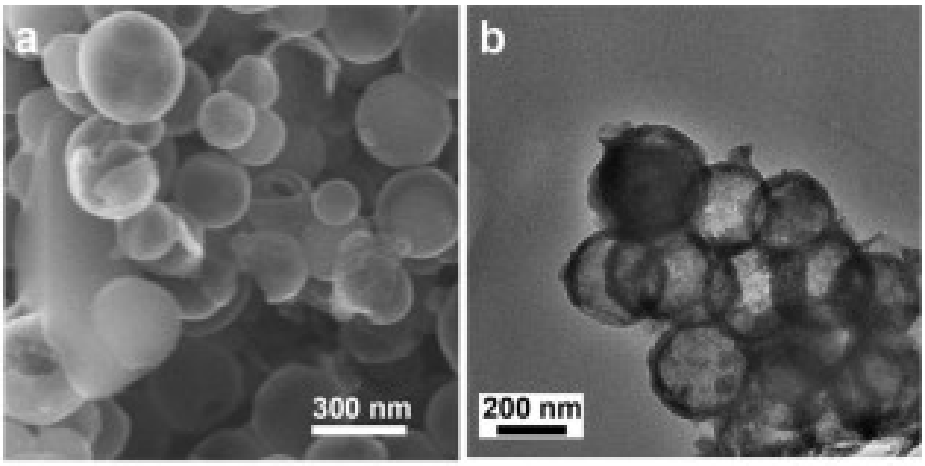

Figure S5. (a) SEM and (b) TEM images of NiPPc/C.

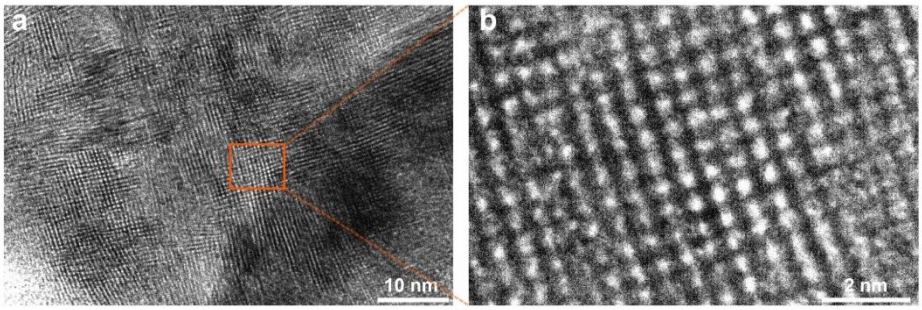

Figure S6. HRTEM images of the NiPPc/C catalyst.

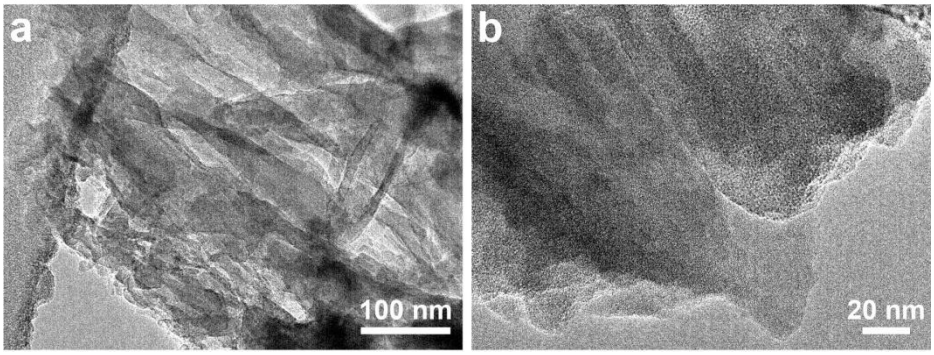

Figure S7. TEM and HRTEM images of the obtained NiPPc catalyst.

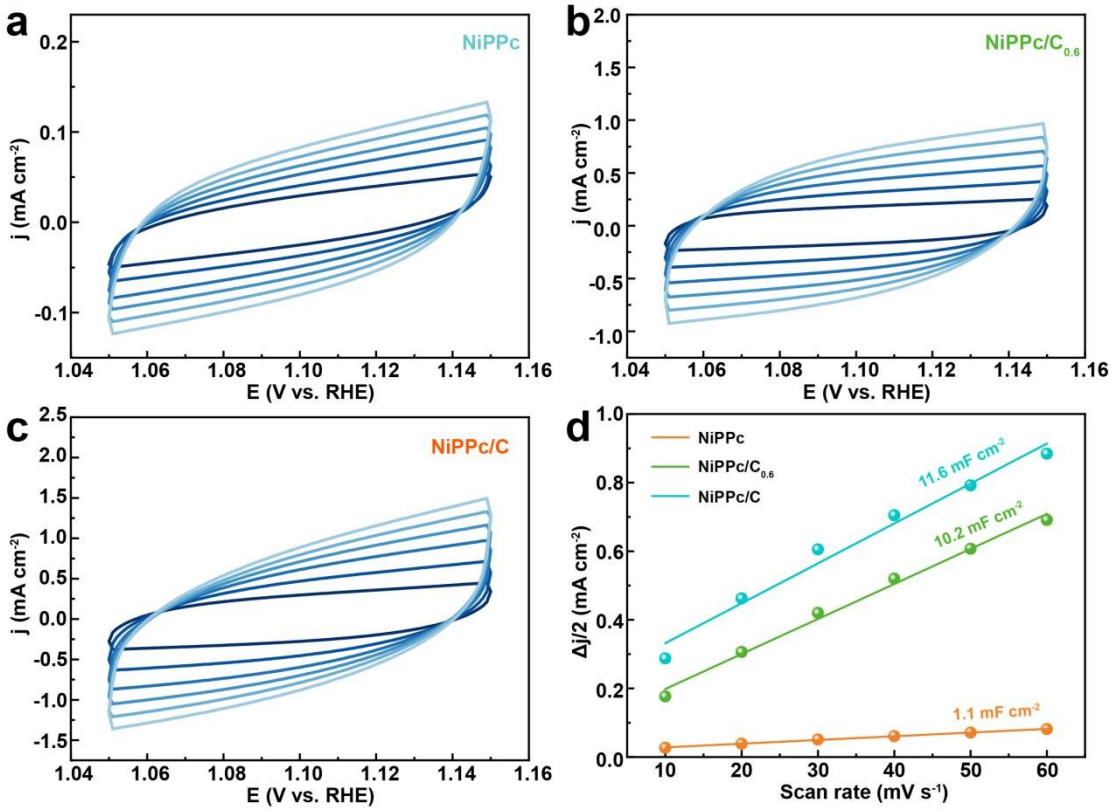

Figure S8. The CV cycles at different scan rates (10-60 mV s^{-1}) for NiPPc, NiPPc/$C_{0.6}$ and NiPPc/C in 1 M KOH with 0.33 M urea electrolyte. (d) Corresponding double-layer capacitance (C_{dl}) via the scan rate-dependent current densities.

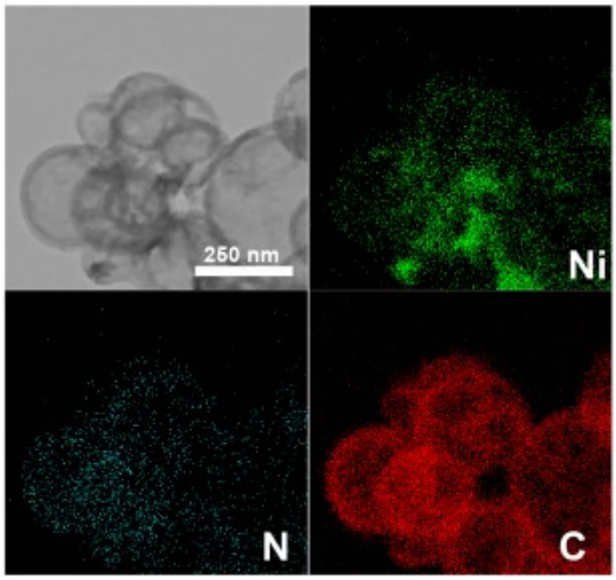

Figure S9. STEM image of NiPPc/C after UOR test and the corresponding EDS mapping of Ni, N and C.

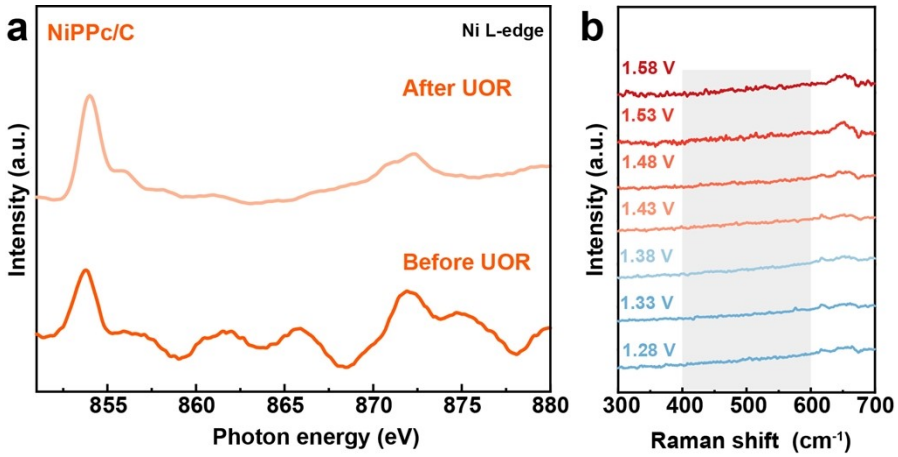

Figure S10. (a) NEXAFS spectra of Ni L-edge of NiPPc/C before and after the UOR. (b) In situ electrochemistry Raman spectra for UOR catalyzed by NiPPc/C, at potential 1.28 to 1.58 V (vs. RHE).

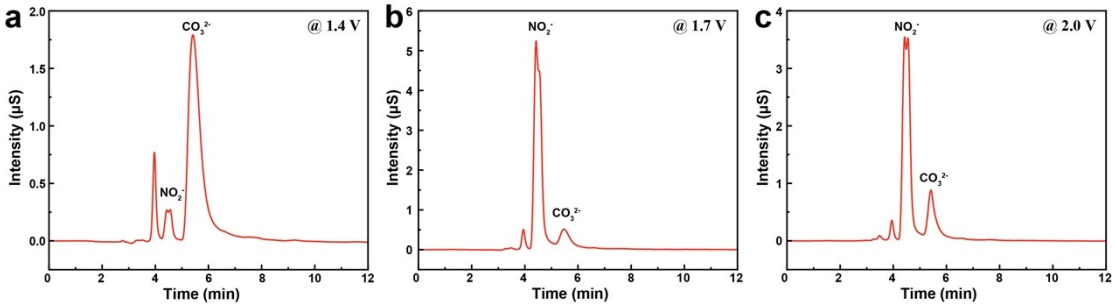

Figure S11. IC curves for electrolytes following UOR catalyzed by NiPPc/C at (a) 1.4 V, (b) 1.7 V and (c) 2.0 V (vs. RHE) for 1 h.

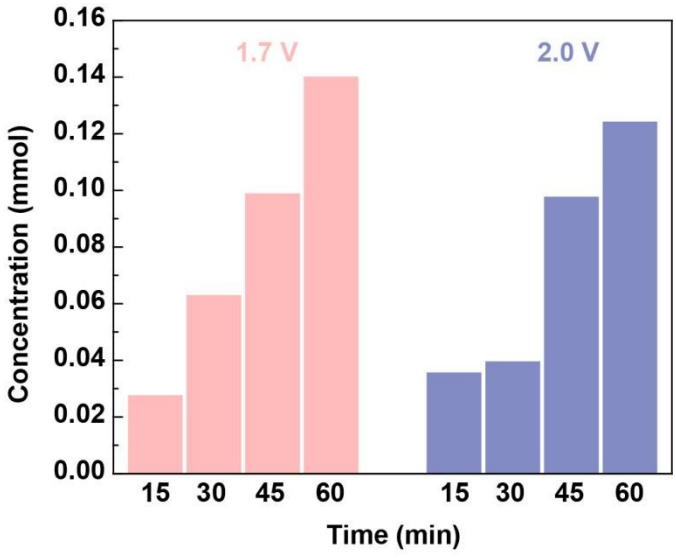

Figure S12. In situ GC for NiPPc/C catalyst to operando monitor N_2 gas during UOR.

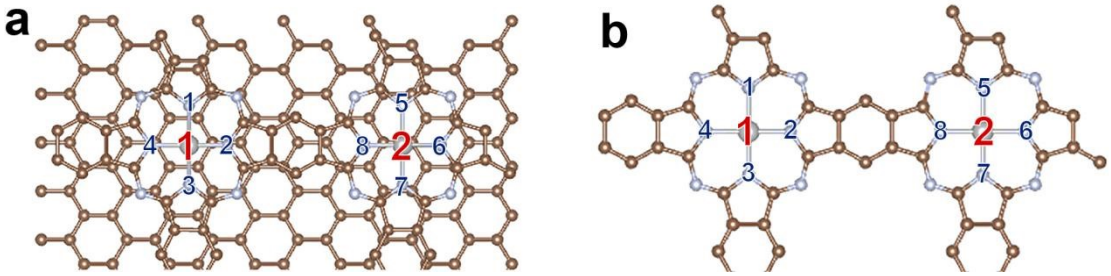

Figure S13. Top views of the structure of NiPPc/C and NiPPc. Ni, grey; N, purple; C, brown.

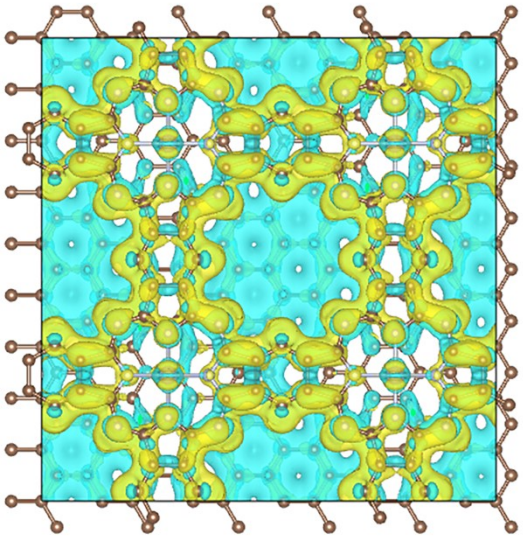

Figure S14. The charge density difference of NiPPc/C.

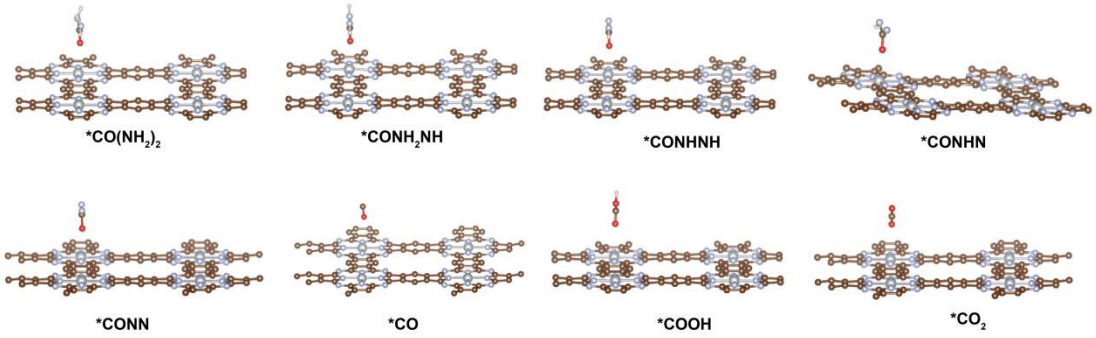

Figure S15. The pathways of UOR on NiPPc.

Table S1. Summary of the potential of non-noble-based electrocatalysts for comparing UOR performance.

Electrocatalysts	Potential (V)@current density (mA cm^{-2})	Tafel slope (mV dec^{-1})	Electrolyte	Ref.
NiPPc/C	1.39@10 1.46@50	30.4	1 M KOH+ 0.33 M urea	This work
Ni-S-Se/N	1.47@10	99.4	1 M KOH+ 0.5 M urea	Nano Energy, 2021, 81, 105605.
Ni/Ni_2P/CNF	1.4@10	37	1 M KOH+ 0.33 M urea	Chem. Commun., 2022, 58(68), 9552-9555.
NiFeMo	1.46@10	43.3	1 M KOH+ 0.33 M urea	Appl. Surf. Sci., 2021, 552, 149514.
Ni-MOF@NiO/Ni-2	1.40@10 1.42@20	48.1	1 M KOH+ 0.33 M urea	Chem. Eng. J., 2021, 417, 129201.
NiCoFe-LTH	1.49@10	43	1 M KOH+ 0.33 M urea	Sustain Energy Fuels, 2022, 6(2), 474-483.
Cu-FMOF-NH_2	1.47@50	105	1 M KOH+ 0.3 M urea	Small, 2023, 19, 2300673.
Fe-MOF/FF-5	1.47@10	20	1 M KOH+ 0.33 M urea	J. Colloid Interface Sci., 2023, 650, 1290-1300.
$NiFe(OH)_x/MnO_2$/NF	1.48@50	53.1	1 M KOH+0.5 M urea	Small, 2024, 20, 2403612.
V-doped $Ni(OH)_2$	1.47@100	29.1	1.0 M KOH+0.33 M urea	Adv. Funct. Mater., 2023, 33, 2209698.
NiF_3/Ni_2P@CC-2	1.45@50	33	1.0 M KOH+0.33 M urea	Chem. Eng. J., 2022, 427, 130865.

Table S2. Comparison of Bader charge between NiPPc/C and NiPPc (Based on the number marked in Figure S8).

Element	Bader Charge (e) of NiPPc/C	Bader Charge (e) of NiPPc
Ni1	-0.892	-0.893
N1	1.078	1.070
N2	1.095	1.102
N3	1.195	1.182
N4	1.057	1.076
Ni2	-0.890	-0.891
N5	1.068	1.068
N6	1.090	1.098
N7	1.194	1.182
N8	1.064	1.100